

Identification of New Fyn Kinase Inhibitors Using a FLAP-Based Approach

Giulio Poli,[†] Tiziano Tuccinardi,^{*,†} Flavio Rizzolio,[‡] Isabella Caligiuri,[‡] Lorenzo Botta,[§] Carlotta Granchi,[†] Gabriella Ortore,[†] Filippo Minutolo,[†] Silvia Schenone,^{||} and Adriano Martinelli[†]

[†]Department of Pharmacy, University of Pisa, 56126 Pisa, Italy

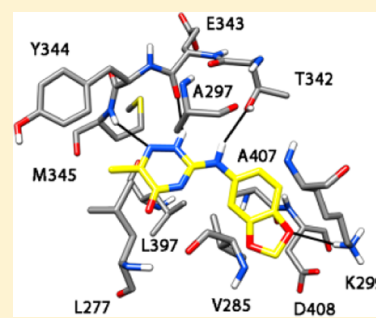
[‡]Division of Experimental and Clinical Pharmacology, Department of Molecular Biology and Translational Research, National Cancer Institute and Center for Molecular Biomedicine, CRO, Aviano, 33081 Pordenone, Italy

[§]Dipartimento Farmaco Chimico Tecnologico, Università di Siena, Via Alcide de Gasperi 2, I-53100 Siena, Italy

^{||}Dipartimento di Scienze Farmaceutiche, Università degli Studi di Genova, Viale Benedetto XV 3, 16132 Genova, Italy

Supporting Information

ABSTRACT: The abnormal activity of Fyn tyrosine kinase has been shown to be related to various human cancers. Furthermore, its involvement in signaling pathways that lead to severe pathologies, such as Alzheimer's and Parkinson's diseases, has also been demonstrated, thus making Fyn an attractive target for the discovery of potential novel therapeutics for brain pathologies and tumors. In this study we evaluated the reliability of various screening approaches based on the FLAP software. By the application of the best procedure, the virtual screening workflow was used to filter the Gold and Platinum database from Asinex to identify new Fyn inhibitors. Enzymatic assays revealed that among the eight top-scoring compounds five proved to efficiently inhibit Fyn activity with IC₅₀ values in the micromolar range. These results demonstrate the validity of the methodologies we followed. Furthermore, the five active compounds herein described may be considered as interesting leads for the development of new and more efficient Fyn inhibitors.



■ INTRODUCTION

Fyn is a cytoplasmic tyrosine kinase (TK) belonging to the Src family of kinases (SFKs). It was identified and characterized in 1988 in both normal and polyoma virus transformed cells.¹ Fyn is involved in several transduction pathways in physiological and pathological situations. In the peripheral immune system it plays important roles in the regulation and in several functions of T-cell development and activation.² Fyn also takes part in several proliferative processes, including cell growth, adhesion, and motility. As a consequence, Fyn overexpression induces morphogenic transformation, alteration of mitogenic signals, and stimulation of cell growth and proliferation, and it is involved in the onset of malignancies.³ In particular, Fyn is overexpressed in breast,^{4,5} ovarian,⁶ prostate,⁷ and pancreatic cancer⁸ and in other tumors,⁹ while very recent studies have shown its involvement in mesothelioma¹⁰ and in chronic myeloid leukemia.¹¹ Furthermore, Fyn inhibition exerts cytoprotective effects by protecting mitochondria and increasing the cellular antioxidant capacity.¹² The Fyn functions that have been most commonly investigated so far, however, are those related to the central nervous system since the enzyme is implicated in brain development processes, such as myelination,¹³ neurite formation in oligodendrocytes,¹⁴ and synapse formation.¹⁵ Moreover, Fyn plays important roles in synaptic transmission and plasticity at excitatory synapses, by interacting with different proteins and receptors, including PSD95

(postsynaptic density protein 95), NMDAR (*N*-methyl-D-aspartate receptor), and AMPAR (α -amino-3-hydroxy-5-methyl-4-isoxazolepropionic acid receptor).¹⁶ Phosphorylation by Fyn of the NMDAR subunit NR2A and Fyn involvement in the interactions between NR2A and PSD95 have been observed after brain ischemia/reperfusion; in fact, increased tyrosine phosphorylation of NR2A and increased interaction between NR2A, PSD95, Src, and Fyn have been detected in ischemic episodes.¹⁷ Fyn has emerged as a regulator of diverse pathological processes. Its hyperactivation/deregulation is involved in neurodegenerative diseases such as Alzheimer's disease (AD) and other tauopathies. These diseases are characterized by the alteration of the Tau protein, a microtubule-associated protein that constitutes a fundamental component of the neurofibrillary tangles of AD.¹⁸ The demonstration that Fyn phosphorylates Tau at its amino terminus on Tyr18 and that tyrosine-phosphorylated Tau is present in the neurofibrillary tangles in the AD brain gives further insights into the involvement of Fyn in tauopathies.¹⁹ Moreover, tyrosine phosphorylation of Tau by Fyn accompanies disease progression.²⁰ This evidence indicates that Fyn is involved in the toxicity mediated by amyloid- β ($A\beta$) oligomers, which are potent synaptotoxins leading to AD-related

Received: April 29, 2013

Published: September 3, 2013

phenotypes.²¹ Fyn is activated by A β oligomers and produces synaptic and cognitive impairment.²² A recent study has also demonstrated that Fyn mediates PSD-95 phosphorylation, which may be responsible for the excitotoxic signal cascades and neuronal apoptosis in brain ischemia and A β neurotoxicity. This study identified a complete signaling cascade linking endogenous A β oligomers, Fyn alteration, and Tau hyperphosphorylation in cellular and animal models of AD.²³ All these new insights confirm that Fyn is a potential therapeutic target for the treatment of malignancies in which it is hyperactivated as well as for treating AD and other tauopathies.

The discovery of selective Fyn kinase inhibitors is of primary importance both for the identification of new drugs and for the obtaining of new tools that might prove to be useful for further investigations on the complex biological pathways in which Fyn is involved. Unfortunately, no specific Fyn inhibitor is available to date since all the known compounds showing Fyn activity are also active at other SFK members or on different TKs. Therefore, the search for selective Fyn inhibitors currently is a hot topic for medicinal chemists. The number of effective Fyn inhibitors is constantly expanding.⁹ Different methods are followed to obtain novel compounds, but the most fruitful one is undoubtedly computer screening. Many docking, QSAR, and 3D-QSAR studies of the c-Src family have been widely published over the few years, and successful virtual screening (VS) studies have been developed.^{24–26} As shown in Figure 1,

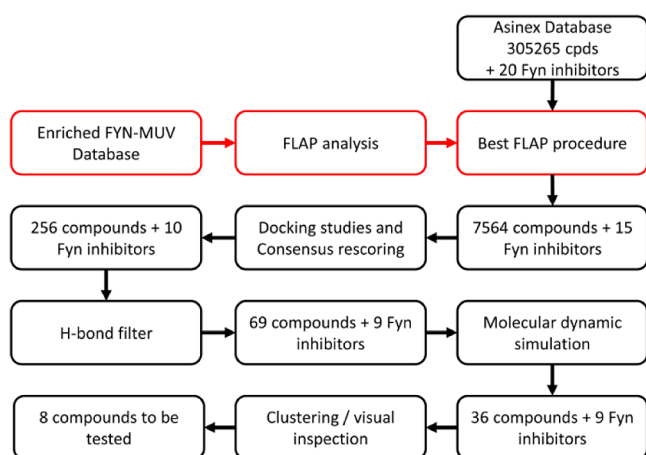


Figure 1. Schematic diagram of the virtual screening workflow.

in the present study, we evaluated the reliability of FLAP software to filter potential Fyn inhibitors. Then, a docking approach combined with molecular dynamic (MD) simulations was carried out to further refine the screening and to identify new potential Fyn inhibitors.

RESULTS AND DISCUSSION

Enriched Virtual Screening Analysis. A classical VS validation takes into consideration a molecular database including a set of molecules that are experimentally validated as active against the selected target, while the rest of the database consists of a large number of compounds presumed to be inactive (decoys). The different VS approaches are then tested for their ability to separate the active molecules from the decoys. To our knowledge, no enriched database consisting of Fyn inhibitors and decoys is presently available in the literature. To build up this database, small molecules for which a Fyn inhibition assay was reported in the literature were analyzed,

and among about 100 compounds identified, 20 compounds showing an IC₅₀ lower than 50 nM were selected as active Fyn inhibitors (see Table S1 in the Supporting Information). As for the choice of suitable decoys from the different available data sets, our attention was focused in particular on the Maximum Unbiased Validation (MUV) Data Sets reported by Rohrer and Baumann in 2009.²⁷ This data set is made up of 18 different databases of 15 030 compounds (30 active and 15 000 decoy molecules) for 18 different targets and among them four targeted kinase enzymes: PKA (cAMP-dependent protein kinase catalytic subunit alpha), FAK (focal adhesion kinase 1), Rho-Kinase2 (Rho-associated protein kinase 2), and Eph rec. A4 (ephrin type-A receptor 4). The decoy data set for PKA was chosen because Fyn and PKA share a very similar shape (see Figure S1 in the Supporting Information), and the binding site is highly conserved with a percentage of identity of 71%. This enriched database of 15 020 compounds, which consisted of the 20 selected Fyn inhibitors and the 15 000 PKA decoys, was then used to validate the VS performance of the software FLAP (Fingerprints for Ligands and Proteins) in separating Fyn actives from decoys. FLAP provides ligand-based, receptor-based, and pharmacophore-based VS approaches through the comparison of common reference frameworks (fingerprints) derived from GRID Molecular Interaction Fields (MIFs) and/or the GRID atom type of small molecules and proteins.²⁸ For this purpose, templates and test compounds need to be processed by the software to create a FLAP database, in which all the information required for calculations is stored for each molecule (see Experimental Section for details). This FLAP database called Fyn-MUV, comprising the whole enriched data set, was then screened by the different FLAP approaches.

FLAP Ligand-Based Virtual Screening. To develop ligand-based analysis, the 20 active Fyn inhibitors were manually clustered into 6 different clusters on the basis of their central scaffold, and one representative compound^{29–34} was selected from each group (see Table 1) to be used as a template for ligand-based screening. The whole data set of 15 020 molecules was thus filtered using, as a template, each of the 6 representative compounds in turn, as well as staurosporine which is the ligand that was cocrystallized in a complex with human Fyn.³⁵

In a ligand-based analysis FLAP compared each template molecule with the whole data set of compounds through the superposition of the MIF-based pharmacophoric features organized in quadruplets. The test compounds were then aligned to the template, based on the best matching quadruplet pairs, and various scores corresponding to the best MIFs overlapping, as well as their combinations, were obtained for each molecule (see Experimental Section for details). The results were evaluated in terms of enrichment factor (EF) for the top 1% and 10% of the ranked database (EF_{1%} and EF_{10%}, respectively) and of area under the enrichment factor curve (AUC). The EF is defined as the fraction of known ligands identified in certain top percentages of the ranked database. At a fixed percentage of the database, the higher the EF, the better the performance of the method in identifying known ligands. The AUC is the area under the curve of the enrichment factor plot (EFP), i.e., the curve defined by all values of EF starting from 0% until 100%; therefore, if the EFP is a diagonal line, the discrimination between actives and decoys is random, and the AUC is 0.5 (corresponding to 50%). In the ideal performance, where all the active known ligands are ranked before all the decoys, the AUC is very close to 1.0 (corresponding to 100%);

Table 1. Representative Fyn Inhibitors Used As Templates for Ligand-Based Screening^{29–34}

1	
2	
3	
4	
5	
6	
7	

therefore, AUC is a measure of the overall performance of a method. As shown in Figure 2, taking into account the AUC and EF factors, the screening using the template compound **5** gave the best statistical results with AUC, EF_{1%}, and EF_{10%} values of 89%, 15%, and 60%, respectively.

FLAP Receptor-Based Virtual Screening. Only one X-ray structure of Fyn complexed with an inhibitor (staurosporine) has so far been reported (2DQ7 PDB code³⁵). Staurosporine was extracted from the X-ray complex, and the protein was

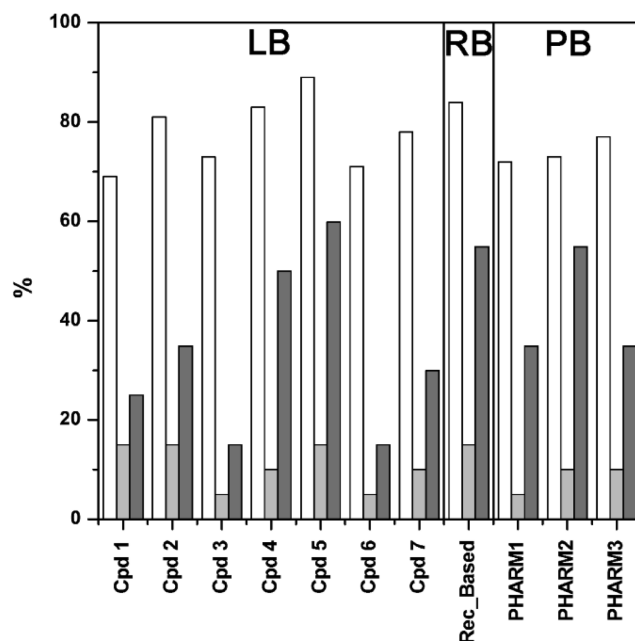


Figure 2. Percentage of AUC (white), EF_{1%} (light gray), and EF_{10%} (gray) values obtained for the enriched Fyn-MUV data set. LB = Ligand-based, RB = receptor-based, and PB = pharmacophore-based approach.

analyzed in terms of binding site detection and MIF calculations. Then the data set of compounds was subjected to FLAP analysis. A receptor-based screen was performed through the superposition of the pharmacophoric quadruplets of template and test compounds, just as in a ligand-based approach. In this case, the template being a receptor site, the matching between the MIF-based quadruplets of the template and the atom-based quadruplets of each small molecule (derived by the combination of its GRID atom types) was analyzed. After their alignment to the receptor, the compounds were scored on the basis of their overlap between the pseudofields (pseudoMIFs), which can be thought of as electron density like fields centered on their heavy atoms, and the protein MIFs (see Experimental Section for details). As shown in Figure 2, the statistical results suggest that this approach was quite reliable for this target with AUC values, EF_{1%}, and EF_{10%}, of 84%, 15%, and 55% of the maximum theoretic value.

FLAP Pharmacophore-Based Virtual Screening. FLAP can also be employed in a pharmacophore-based approach through the FLAPpharm tool.³⁶ Figure 3 shows the three different pharmacophoric models generated (PHARM1–3). These models were those associated to the highest score, which

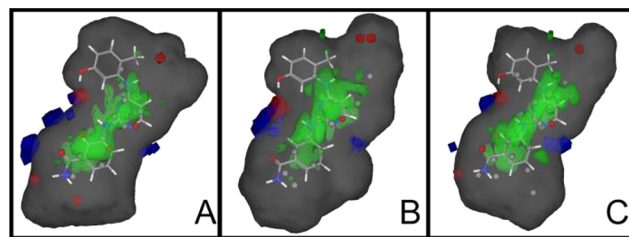


Figure 3. FLAP pharmacophoric models (A) PHARM1; (B) PHARM2; and (C) PHARM3 overlapped to compound **5** as a reference structure.

were generated by aligning the seven representative Fyn active compounds (1–7, Table 1). A FLAP pharmacophoric model is defined as a pseudomolecule identified by a pattern of atom-based pharmacophoric points, derived from the common atomic locations of the aligned compounds as well as of field-based pharmacophoric points representing the hotspots obtained by the condensation of the PIFs (pharmacophore interaction fields, corresponding to the common shared portions of the MIFs of the aligned compounds). Therefore, a pharmacophore-based VS can be performed through the superposition of the MIF-based quadruplets of the test molecules with the PIF-based quadruplets of the template pharmacophoric model, and the scores are calculated on the basis of the overlap between MIFs and PIFs of aligned compounds and model, respectively (see Experimental Section for details). Among the three best scored pharmacophoric models PHARM1–3, which were obtained by the software and were used for VS, the second model (PHARM2) displayed the best overall results after statistical analysis, with AUC, EF_{1%}, and EF_{10%} values of 73%, 10%, and 55%, respectively (Figure 2).

The FLAP analysis of the enriched database consisting of Fyn active inhibitors together with the PKA1MUV decoys suggests that, although positive results were obtained for all three tested procedures, the ligand-based approach appears to be the best one for screening Fyn inhibitors, and in particular, the use of compound 5 as the query structure gave the best statistical results (Figure 4A).

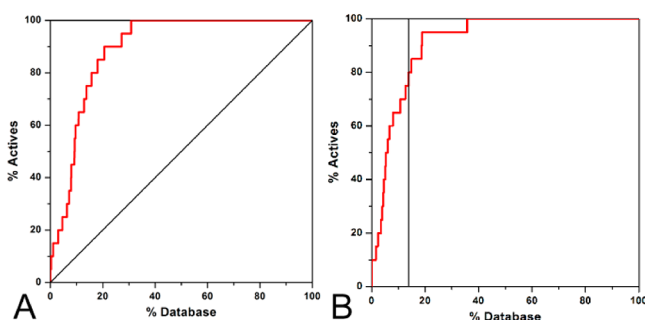


Figure 4. Filtering results for the Fyn enriched database (A) and the Asinex database (B) using compound 5 as the query structure for the FLAP ligand-based analysis. In plot B the threshold used for the virtual screening is showed.

Virtual Screening Studies. The Asinex database (gold and platinum databases) was enriched with the 20 known active Fyn inhibitors. The whole database was then subjected to the FLAP filtering by using the procedure that showed the best results for the Fyn-MUV database, i.e., the ligand-based approach with compound 5 as the query structure. Prior to the full calculation, a bit-string filtering was carried out to reduce the number of compounds to be analyzed. Then conformational ensemble generations were developed using FLAP, and the database thus obtained was submitted to the ligand-based filtering. Among the 20 known active Fyn inhibitors, four compounds were characterized by the presence of a 5,6-dihydrobenzo[*h*]quinazoline central scaffold (compounds 2, 9, 11, and 12 in Table S1, Supporting Information). The FLAP filtering was able to discriminate among these compounds as compounds 9, 11, and 12 were ranked in the top 50%, whereas compound 2 was discarded as it was ranked

outside the 80% threshold; therefore, FLAP filtering seems to be able to discriminate among similar compounds.

Overall, the statistical analysis confirmed the reliability of this method since the results obtained were very similar to the results obtained by using the Fyn-MUV database, with AUC, EF_{1%}, and EF_{10%} values of 91%, 10%, and 65%, respectively. As shown in Figure 4B, all the ligands having scoring values in the range of that showed by 80% of the known active molecules were taken into account, resulting in 7564 compounds. The filtered database was then subjected to docking studies. This step was carried out by means of the GOLD software³⁷ by using the ChemPlp scoring function, as it proved to be one of the best methods for docking kinase inhibitors.³⁸ The docked molecules were then ranked by using two scoring functions, Chemscore from Fred³⁹ and Amberscore from Dock 6.0⁴⁰ (see Figure S2 in the Supporting Information), which resulted to be the best performing method among the various different scoring functions that were tested. The compounds predicted as active were the ones showing a scoring value in the range of the first 80% of the active molecules by both these scoring functions. On these bases, 256 compounds were considered as active and, therefore, taken into account. It is well-known from the analysis of X-ray complexes between kinases and inhibitors interacting in their ATP binding site^{41,42} that the backbone nitrogen of residue 345, which corresponds to a methionine in the Fyn, and the backbone oxygen of E343 and M345 play important roles in the binding process since they usually form key hydrogen bonds with this type of inhibitor. Furthermore, an in-house analysis of about 500 ligands crystallized with kinases revealed that more than 90% of deposited compounds showed H-bond interactions with the kinase hinge region. On these bases, the interaction with the kinase hinge region appears to be very important, even if novel binders could also be characterized by the absence of this interaction. As a result, in the postscoring step, all the compounds that did not form at least two H-bonds with the backbone nitrogen of M345 and with the backbone oxygen of E343 and M345 were rejected, and the resulting 69 compounds were then subjected to a MD simulation with the aim of verifying the stability of the inhibitor–enzyme interactions. To set up the MD simulation protocol, the complex between staurosporine and human Fyn (2DQ7 PDB code³⁵) was used as a test. The residues beyond a threshold of 12 Å from the ligand were removed, and as a result, only the segments L270–L350 and R392–L411 were considered (see Figure S3 in the Supporting Information) and solvated with a 10 Å water cap (see Experimental Section for more details). The ligand–protein complex was then subjected to a total of 2 ns of MD simulation. As shown in Figure S4 in the Supporting Information, the system reached an equilibrium after about 400 ps since the total energy for the last 1.6 ns remained approximately constant. By analyzing the root-mean-square deviation (RMSD) of all the heavy atoms from the X-ray structures, we observed an initial increase due to the equilibration of the system, followed, after about 600 ps, by a stabilization of the RMSD value around 1.5 Å. Regarding the geometry of the ligand, we analyzed the RMSD of the position of the ligand with respect to the X-ray structure during the simulation, and it shows an RMSD value around 0.3 Å (Figure S4, Supporting Information). With regard to the H-bond analysis (Table S2 in the Supporting Information), the interaction of the ligand with the backbone nitrogen of M345 and the backbone oxygen of E343 system appears to be very

stable, as these interactions were maintained during almost the whole MD process.

The 69 compounds obtained by the previous VS steps were subjected to MD simulation using the same protocol described above, and all the ligands that maintained the H-bonds with the backbone atoms of E343 and M345 for at least 90% of the whole MD simulation were kept for further consideration. About 50% of the compounds were rejected by using this filter, and the remaining 36 compounds were visually checked and clustered on the basis of their central scaffold. Eight different scaffolds were identified, and thus eight representative compounds were chosen. The relatively small number of clusters identified was due to the fact that 19 out of the 36 molecules shared a quinolinone scaffold and were therefore clustered together and represented by compound VS3 (Table 2). The other 7 scaffolds were identified by analyzing the remaining 17 compounds.

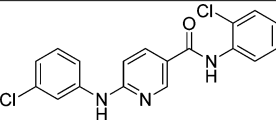
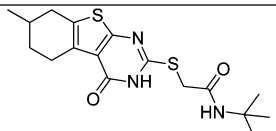
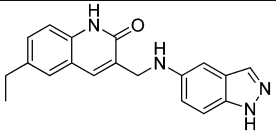
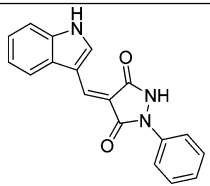
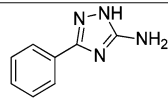
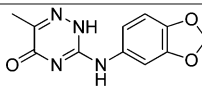
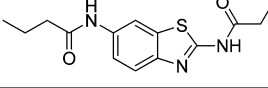
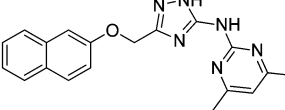
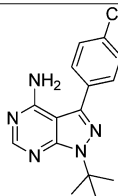
To test the reliability of the VS protocol from an experimental point of view, these compounds of the Asinex database, that were predicted to be high affinity Fyn inhibitors, were purchased and subjected to a Fyn inhibition assay (see the Experimental Section for details), together with the reference Src inhibitor PP2⁴³ that was used as a positive control. As indicated in Table 2, five out of the eight compounds showed appreciable Fyn inhibitory activities with IC₅₀ values ranging from 5 to 71 μ M, corresponding to a hit ratio of 62.5%.

As shown in Figure 5A, the binding hypothesis for the 6-aminonicotinamide central scaffold of compound VS1 suggests the presence of two H-bonds with the backbone of M345 and an additional H-bond with the hydroxyl group of T342; the 3-chlorophenyl ring is directed toward the solvent-accessible region of the binding site, and on the other side, the antipodal 2-chlorophenyl ring mainly interacts with V285 and the methyl group of T342. Figure 5B shows the minimized average structure of compound VS3 docked into Fyn, where the quinolinone central scaffold forms two H-bonds with the backbone of M345 and the indazole group forms a H-bond with the nitrogen backbone of D408 and interacts with V285 and L397. With regard to compound VS4, the phenyl ring is directed toward the solvent-accessible region of the binding site; the pyrazolidine system shows two H-bonds with the backbone of M345; and the indole ring forms a H-bond with the hydroxyl group of T342 and interacts with V285 and L397 (see Figure 5C). As shown in Figure 5D, the triazinone central scaffold of compound VS6 interacts with the nitrogen backbone of M345 and the oxygen backbone of E343; furthermore, the amine function forms a H-bond with the hydroxyl group of T342, and the benzodioxole ring shows a secondary H-bond with K299. Finally, as shown in Figure 5E, the naphthalene ring of compound VS8 is directed outside the binding site region; the triazole ring forms a H-bond with the nitrogen backbone of M345 and another one with the oxygen backbone of E343; whereas the substituted 2-pyrimidinamine portion interacts with V285 and forms a H-bond with the hydroxyl group of T342.

A similarity search for compounds VS1, VS3, VS4, VS6, and VS8 against the already published kinase ligands revealed that, with the exception of compound VS4 that had already been reported as a protein tyrosine kinase inhibitor,⁴⁴ there are no kinase ligands with a similarity score greater than 80 (score = 100 means that the two compounds are identical).

To provide an overall computational validation of the applied screening protocol, the 19 known Fyn active inhibitors were

Table 2. Structure and Fyn Activity of the Compounds Tested

	Compd. Structure	Code	IC ₅₀ (μ M) ^a
VS1		ASN 05346611	71.2
VS2		ASN 06152825	> 500
VS3		ASN 07404571	15.0
VS4		BAS 00244777	11.5
VS5		BAS 01171840	> 500
VS6		BAS 04199656	4.8
VS7		BAS 12987897	> 500
VS8		BAS 14602180	46.7
		PP2	0.063

^aIC₅₀ values represent the concentration required to produce 50% enzyme inhibition. Values are the average from at least two independent dose–response curves.

subjected to the whole screening workflow (compound 5 was not included as it was used as the query structure for the FLAP filtering step). As shown in Figure 1, among the 15 compounds filtered by the FLAP ligand-based procedure, 10 compounds were predicted as active by both Chemscore and Amberscore scoring functions and of these compounds, and only one was rejected because its docking pose did not form at least two H-bonds with the backbone nitrogen of M345 and with the backbone oxygen of E343 and M345. Finally, all the resulting nine compounds maintained the H-bond interactions with the backbone atoms of these residues for at least 90% of the whole

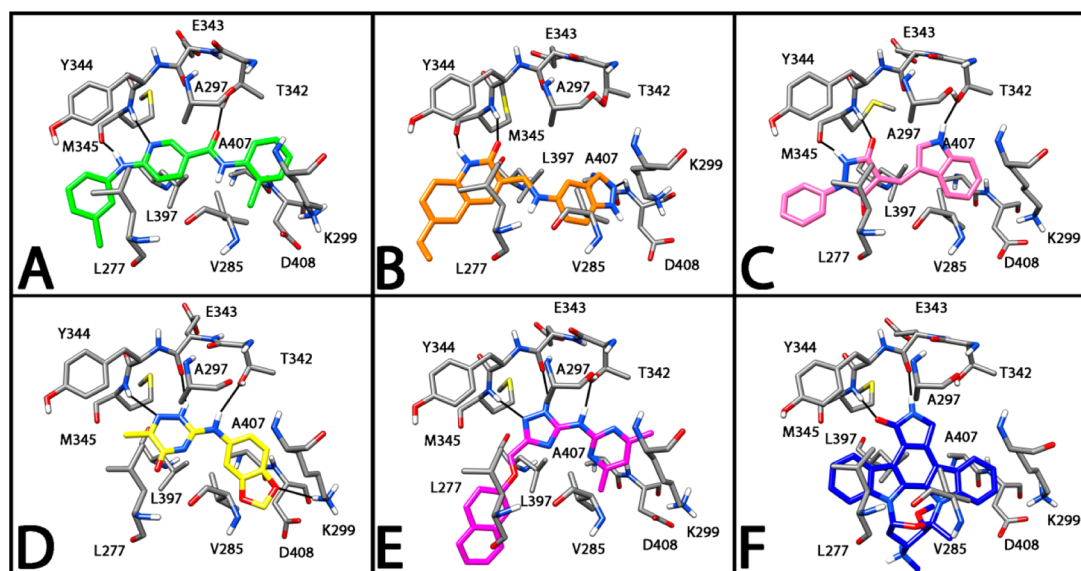


Figure 5. Minimized average structures of compounds VS1 (A), VS3 (B), VS4 (C), VS6 (D), and VS8 (E) docked into Fyn. The X-ray complex between Fyn and staurosporine is also reported as a reference system (F).

MD simulation, resulting in a high enrichment factor (EF) value (EF = 3213, see the Experimental Section for a brief description of this measurement).

Selectivity and Cellular Assays. To better evaluate the lead characteristics of the reported molecules, compounds VS3, VS4, and VS6 were screened against a small panel of different kinases. As shown in Figure 6, compound VS3 does not

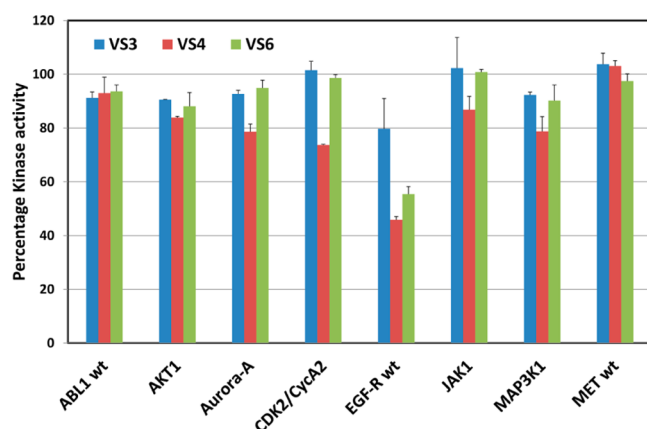


Figure 6. Percent kinase activity observed at 20 μM concentration of the tested compounds. Values are the average from two evaluations. Error bars indicate standard error of the mean.

highlight activity against any of the tested kinases, whereas VS4 and VS6 show activity against the Epidermal Growth Factor Receptor (EGFR). A superimposition between the Fyn and EGFR binding sites (see Figure S5 in the Supporting

Information) highlights the high level of similarity between the two sites, with only E343, Y344, and A407 that are not conserved (substituted by Q791, L792, and T854 in the human EGFR, respectively). For the future lead optimizations of the reported compounds, this aspect will be taken into account for the improvement of the ligand selectivity.

The three Fyn inhibitors showing the best activity in the enzymatic assay (compounds VS3, VS4, and VS6) were selected to be further tested in *in vitro* experiments to evaluate their antiproliferative potencies on cancer cells. To this aim, two tumor cell lines were chosen, the highly invasive human breast MDA-MB-231 and the human nonsmall-cell lung A549 cancer cells, due to the critical role that Fyn plays in the tumor progression and development of metastases in these kinds of tumors.^{4,45,46} Overall, all three compounds produced an appreciable inhibition of cell viability, with IC_{50} values ranging from 62.7 to 198.2 μM (see Table 3). Furthermore, all compounds were shown to be significantly less potent against noncancerous human fetal lung fibroblast cells (MRC-5, Table 3).

Refinement of the Virtual Screening Workflow. The interaction of the best ranked pose of the ligands belonging to the database with the hinge region of the Fyn kinase represented one of the key steps of our VS procedure. However, by applying this rule, if a compound was discarded at this step, there could have been another of the 30 docking poses interacting with the hinge region and scoring nearly as well as the docking pose that was discarded. To optimize this step a second VS study was carried out starting from the 7564 compounds selected by means of FLAP. These compounds were then docked as described above, and for each compound

Table 3. Cell Growth Inhibitory Activities (IC_{50}) of Compounds VS3, VS4, VS6, and PP2

cancer cell line	tissue of origin	IC_{50} values (μM)			
		VS3	VS4	VS6	PP2
A549	lung	117.7 \pm 13.9	100.1 \pm 17.5	145.0 \pm 13.3	7.0 \pm 1.7
MDA-MB-231	breast	136.4 \pm 17.5	62.7 \pm 13.1	198.2 \pm 9.1	14.9 \pm 4.7
MRC-5	normal fibroblast	>300	>300	>300	30.6 \pm 4.0

all the 30 generated docking poses were taken into account, for a total of 226 920 poses. This data set was then filtered by removing all the poses that did not form at least two H-bonds with the Fyn kinase hinge region, resulting in 15 603 docking poses, and then filtered by means of the rescoring using Chemscore from Fred³⁹ and Amberscore from Dock 6.0⁴⁰ as described above. This filter resulted in the selection of 788 poses that corresponded to 151 compounds that were then subjected to a total of 2 ns of MD simulation. All the ligands that maintained the H-bonds with the backbone atoms of E343 and M345 for at least 90% of the whole MD simulation were kept for further consideration. About 50% of the compounds were rejected by using this filter, and the remaining 70 compounds were visually checked and clustered on the basis of their central scaffold. Beyond the eight clusters already identified, this analysis led to the identification of four new cluster compounds (see Table S3 in the Supporting Information) that will be evaluated for their activity against Fyn, to experimentally verify the reliability of this optimization of the VS procedure.

CONCLUSIONS

In the present work, we tested the application of a FLAP-based method for the development of a VS study for Fyn inhibitors. First of all, we analyzed the ability of FLAP to filter an enriched database. The best procedure was then used to filter a commercial database of about 300 000 commercial compounds, and the results were further filtered by using a combined approach that includes docking calculations, rescoring evaluation, and MD simulations. To experimentally verify the reliability of this procedure, eight compounds from the commercial database, which were predicted to be active by the above-mentioned VS study, were tested for their inhibitory potency against Fyn. Five compounds out of the eight tested showed IC₅₀ values in the micromolar range; moreover, the three most active compounds showed appreciable cell growth inhibitory activities in an antiproliferative assay carried out on two cancer cell lines. Taken together, these findings suggest that the optimized techniques herein reported may be suitable for the identification of new Fyn inhibitors and encourage us to apply this method to other compound databases. Furthermore, the reported screened compounds could already be considered as leads for the development of new active Fyn inhibitors.

EXPERIMENTAL SECTION

Database Generation. The Asinex database and the MUV set of decoys for PKA1 were enriched with 20 known active Fyn inhibitors and subjected to the database generation protocol implemented in FLAP. This process can be divided into five different steps: (a) a conformational sampling (and optionally protomers, tautomers, and stereoisomers search) is carried out, and an appropriate number of conformers is saved for each molecule; (b) the Molecular Interaction Fields (MIFs) relative to the user-defined probes are generated and stored for each compound conformer through the GRID force field, to evaluate the type, the strength, and the spatial localization of the possible interactions that the molecule can establish; (c) the MIFs of each compound conformer are condensed into discrete pharmacophoric points representing the most favorable interaction locations; (d) all the possible 4-point pharmacophores obtained through the combination of these discrete points (the MIF-based quadruplets) are then generated; (e) all

the MIF-based quadruplets generated for each conformer of each molecule are then saved, constituting the compound fingerprints that will be used for calculations in VS approaches. For the creation of the two databases, the most populated tautomer at pH 7.4 of each compound was used. Conformational analyses were carried out using a random search, retaining up to 50 conformers per molecule while eliminating those with an RMSD < 0.2 Å from any other. The initial conformer of each compound was generated using the LigPrep software,⁴⁷ which performs a series of steps that perform conversions, apply corrections to the structures, eliminate unwanted structures, and optimize the structures. For the MIF generation, the GRID probes H, DRY, N1, and O (shape, hydrophobic, H-bond donor, H-bond acceptor) were used, with a grid resolution of 0.70 Å. The choice of such grid resolution value was guided by the settings used by Cross and co-workers for the validation of FLAP software by using the DUD data set.⁴⁸ All the other settings were left as their defaults.

FLAP Virtual Screening Analyses. *FLAP Ligand-Based Virtual Screening.* All the ligand-based virtual screenings were carried out by selecting from the database the appropriate active Fyn inhibitor to be used as a template for the calculation and leaving the other settings as their defaults.

FLAP Receptor-Based Virtual Screening. The only X-ray structure of Fyn catalytic domain available in the literature was used as a template for the receptor-based VS after stripping the water and extracting the bound ligand (staurosporine) from the X-ray complex (PDB code 2DQ7). The kinase domain was thus imported into FLAP and fixed by applying the FLAP default basic filters for pdb files. The FLAPsite algorithm⁴⁹ was then applied for the identification of the protein cavities, and the bound ligand was imported to check its location within the best ranked pocket, corresponding to the kinase catalytic site, that was used as a template for the receptor-based VS. The calculation was carried out leaving the parameters as their defaults except for the max minima point that was set to 100, so that 100% of the discrete pharmacophoric points in which the protein MIFs are condensed were used for quadruplet alignment.

FLAP Pharmacophore-Based Virtual Screening. The FLAPPharm tool of the FLAP algorithm was used for the pharmacophore model generation. The six representative Fyn active compounds, selected from the FLAP database, were used as input structures for the alignment that was carried out by setting the yielding of the three best ranked pharmacophore models and leaving the other settings as their defaults. All the pharmacophore-based VSs were carried out by selecting one of the three generated models as a template and leaving the other settings as their defaults. For each pharmacophore model FLAPPharm calculates a score that is then used for ranking the different models. To achieve this, FLAPPharm has been parametrized with a single global scoring function that is a weighted sum of the shape, hydrogen-bond donor, acceptor, and hydrophobic MIFs.

Docking Studies. Automated docking was carried out by means of the GOLD program, version 4.1.1.³⁷ The region of interest for the docking studies was defined in such a manner that it contained all residues within 10 Å of the staurosporine ligand in the X-ray crystal structure (2DQ7 PDB code). The “allow early termination” command was deactivated, while the possibility for the ligand to flip ring corners was activated. The remaining GOLD default parameters were used, and the ligands were submitted to 30 genetic algorithm runs by applying the

PLP fitness function. We decided to use this software with this procedure since our previous cross-docking studies on kinases suggested that this protocol was one of the most reliable for docking kinase ligands.³⁸ The best docked conformation was taken into account. The docking results were then scored by means of different rescoring functions, and among them the use of ChemScore from Fred 2.2.5³⁹ and Amber from Dock 6.0⁴⁰ resulted to be the most reliable. All the default parameters were applied when using these scoring functions.

Molecular Dynamic Simulations. All simulations were performed using AMBER 11.⁵⁰ Starting from the crystal structure of human Fyn complexed with staurosporine, the residues beyond a threshold of 12 Å from the ligand were removed, and as a result only the segments L270–L350 and R392–L411 were considered. The complexes were placed in a rectangular parallelepiped water box; an explicit solvent model for water (TIP3P) was used; and the complexes were solvated with a 10 Å water cap. Chlorine ions were added as counterions to neutralize the system. Two steps of minimization were then carried out. In the first stage, we kept the complexes fixed with a position restraint of 500 kcal/(mol·Å²), and we solely minimized the positions of the water molecules. In the second stage, we minimized the entire system through 20 000 steps of steepest descent followed by conjugate gradient until a convergence of 0.05 kcal/(mol·Å²) was attained. All the α carbons of the protein were blocked with a harmonic force constant of 10 kcal/(mol·Å²). Two nanoseconds of MD simulation were then carried out. The time step of the simulations was 2.0 fs with a cutoff of 10 Å for the nonbonded interaction, and SHAKE was employed to keep all bonds involving hydrogen atoms rigid. Constant-volume periodic boundary MD was carried out for 300 ps, during which the temperature was raised from 0 to 300 K. Then 1.7 ns of constant pressure periodic boundary MD was carried out at 300 K by using the Langevin thermostat to maintain the temperature of our system constant. General Amber force field (GAFF) parameters were assigned to the ligands, while partial charges were calculated using the AM1-BCC method as implemented in the Quacpac software from Openeye.⁵¹

Virtual Screening Evaluation. The VS result was evaluated by using the Enrichment factor.⁵² It measures the enrichment of the method compared with random selection

$$EF = [t_p / (t_p + f_n)](NC_{tot} / NC)$$

where t_p is the number of high affinity compounds not rejected (true positives); f_n is the number of high affinity compounds rejected during the VS filtering (false negatives); NC_{tot} is the total number of molecules of the database ($NC_{tot} = 305\,265 + 19$); and NC is the total number of compounds obtained at the end of the VS protocol ($NC = 36 + 9$).

Similarity Search. The test compounds were compared with published kinase ligands. This comparison was made by using the Similarity Search task of SciFinder.⁵³ Similarity search locates structures that are similar to the query, based on a two-dimensional small-molecule comparison using a Tanimoto similarity metric. A score of 100 means that the two structures are identical.

Fyn Kinase Assays. Eight compounds selected by VS were purchased from Asinex.⁵⁴ PP2 was purchased by Tocris Bioscience.⁵⁵ Full-length recombinant human Fyn, Poly (Glu4,Tyr1) synthetic peptide substrate, ATP stock solution, and Kinase-Glo Luminescent Kinase Assay were from Promega.⁵⁶ The IC_{50} values for compounds were generated

in 96-well microtiter plates by using the Kinase-Glo Luminescent Kinase Assay. The kinase reaction was conducted at room temperature at a final volume of 50 μ L in 40 mM Tris buffer, pH 7.5, containing 20 mM MgCl₂ and 0.05 mM DTT. A total of 10 μ L of ATP 20 μ M was added to 10 μ L of Poly (Glu4,Tyr1) synthetic peptide substrate 1 μ g/ μ L and 5 μ L of DMSO containing the appropriate amount of compound. The reaction was initiated by the addition of 25 μ L of Fyn (36–48 ng/well) in such a way that the assay was linear over 60 min. The final concentration of the analyzed compounds ranged for PP2 from 10 to 0.032 μ M and for the VS compounds from 500 to 0.8 μ M. After the reaction had proceeded for 60 min, 50 μ L of Kinase-Glo reagent was added to terminate the reaction. This solution was then allowed to proceed for an additional 10 min to maximize the luminescence reaction. Values were then measured by using a VictorX3 PerkinElmer instrument for luminosity measurements. Two reactions were also run: one reaction containing no compounds and the second one containing neither inhibitor nor enzyme. IC_{50} values were derived from experimental data using the Sigmoidal dose–response fitting of Prism (Version 3; GraphPad Software). To remove possible false positive results that could be caused by the presence of fluorescent ligands or compounds with inhibitory activity versus Kinase-Glo reagent, for each compound concentration a blank analysis was carried out, and the final fluorescence results were obtained deducting the fluorescence produced by the presence of all the components except Fyn in the same conditions.

Protein Kinase Assay. The screening against the kinase panel was carried out by ProQinase GmbH.⁵⁷ A radiometric protein kinase assay (³³PanQinase Activity Assay) was used for measuring the kinase activity of the 8 protein kinases. All kinase assays were performed in 96-well FlashPlates from Perkin-Elmer (Boston, MA, USA) in a 50 μ L reaction volume. The assay for all protein kinases contained 70 mM HEPES-NaOH pH 7.5, 3 mM MgCl₂, 3 mM MnCl₂, 3 μ M Na-orthovanadate, 1.2 mM DTT, ATP (variable amounts, corresponding to the apparent ATP-K_m of the respective kinase), [γ -³³P]-ATP (approximately 5 \times 1005 cpm per well), protein kinase, and substrate. The reaction cocktails were incubated at 30 °C for 60 min. The reaction was stopped with 50 μ L of 2% (v/v) H₃PO₄, and plates were aspirated and washed two times with 200 μ L of 0.9% (w/v) NaCl. Incorporation of ³³P_i (counting of “cpm”) was determined with a microplate scintillation counter (Microbeta, Wallac). All assays were performed with a BeckmanCoulter Biomek 2000/SL robotic system. The inhibitory activity of the selected compounds was assayed by adding 5 μ L of the inhibitor solution to the reaction mixture described above. All the compounds were dissolved in 100% DMSO and diluted for reaching a final concentration of 20 μ M.

Cell Viability Assay. MDA-MB-231 (human breast carcinoma cells), A549 (non-small cell lung cancer), and normal cells (MRC-5) were purchased from ATCC and maintained at 37 °C in a humidified atmosphere containing 5% CO₂ accordingly to the supplier. Normal (3×10^4) and tumor (10^3) cells were plated in 96-well culture plates. The day after seeding, vehicle or compounds were added at different concentrations to the medium. Fyn inhibitors VS3, VS4, and VS6 were added to the cell culture at a concentration ranging from 400 to 0.1 μ M. Differently, PP2 was added to the cell culture at a concentration ranging from 200 to 0.02 μ M. Cell viability was measured after 72 h according to the supplier (Promega, G7571) with a Tecan F200 instrument. IC_{50} values

were calculated from logistical dose response curves. Averages were obtained from three independent experiments, and error is standard error ($n = 3$).

■ ASSOCIATED CONTENT

■ Supporting Information

Known active Fyn inhibitors, H-bond analysis of the staurosporine–Fyn complex, and representative compounds belonging to the new four clusters identified by means of the VS workflow refinement (Table S1, S2 and S3); superimposition between Fyn and PKA kinase, rescoring results of the filtered enriched database after docking calculations, superimposition between the X-ray structure of Fyn kinase and the region used for the MD simulations, analysis of the MD simulation of staurosporine complexed with Fyn kinase; and superimposition between Fyn and EGFR binding site. This material is available free of charge via the Internet at <http://pubs.acs.org>.

■ AUTHOR INFORMATION

Corresponding Author

*Phone: +39 0502219595. E-mail: tiziano.tuccinardi@farm.unipi.it.

Notes

The authors declare no competing financial interest.

■ ACKNOWLEDGMENTS

Financial support for this project was provided by the Italian Ministero dell'Università e della Ricerca (MIUR), under the National Interest Research Projects framework (PRIN_2010_SY2HL).

■ REFERENCES

- (1) Kypta, R. M.; Hemming, A.; Courtneidge, S. A. Identification and Characterization of P59fyn (a Src-Like Protein Tyrosine Kinase) in Normal and Polyoma-Virus Transformed-Cells. *EMBO J.* **1988**, *7*, 3837–3844.
- (2) Salmond, R. J.; Filby, A.; Qureshi, I.; Caserta, S.; Zamoyska, R. T-cell receptor proximal signaling via the Src-family kinases, Lck and Fyn, influences T-cell activation, differentiation, and tolerance. *Immunol. Rev.* **2009**, *228*, 9–22.
- (3) Saito, Y. D.; Jensen, A. R.; Salgia, R.; Posadas, E. M. Fyn A Novel Molecular Target in Cancer. *Cancer* **2010**, *116*, 1629–1637.
- (4) Kostic, A.; Lynch, C. D.; Sheetz, M. P. Differential Matrix Rigidity Response in Breast Cancer Cell Lines Correlates with the Tissue Tropism. *PLoS One* **2009**, *4*, e6361.
- (5) Charpin, C.; Secq, V.; Giusiano, S.; Carpentier, S.; Andrac, L.; Lavaut, M. N.; Allasia, C.; Bonnier, P.; Garcia, S. A signature predictive of disease outcome in breast carcinomas, identified by quantitative immunocytochemical assays. *Int. J. Cancer* **2009**, *124*, 2124–2134.
- (6) Huang, R. Y. J.; Wang, S. M.; Hsieh, C. Y.; Wu, J. C. Lysophosphatidic acid induces ovarian cancer cell dispersal by activating Fyn kinase associated with p120-catenin. *Int. J. Cancer* **2008**, *123*, 801–809.
- (7) Posadas, E. M.; Al-Ahmadie, H.; Robinson, V. L.; Jagadeeswaran, R.; Otto, K.; Kasza, K. E.; Tretiakov, M.; Siddiqui, J.; Pienta, K. J.; Stadler, W. M.; Rinker-Schaeffer, C.; Salgia, R. FYN is overexpressed in human prostate cancer. *BJU Int.* **2009**, *103*, 171–177.
- (8) Chen, Z. Y.; Cai, L.; Zhu, J.; Chen, M.; Chen, J.; Li, Z. H.; Liu, X. D.; Wang, S. G.; Bie, P.; Jiang, P.; Dong, J. H.; Li, X. W. Fyn requires HnRNPA2B1 and Sam68 to synergistically regulate apoptosis in pancreatic cancer. *Carcinogenesis* **2011**, *32*, 1419–1426.
- (9) Schenone, S.; Brullo, C.; Musumeci, F.; Biava, M.; Falchi, F.; Botta, M. Fyn Kinase in Brain Diseases and Cancer: The Search for Inhibitors. *Curr. Med. Chem.* **2011**, *18*, 2921–2942.
- (10) Eguchi, R.; Kubo, S.; Takeda, H.; Ohta, T.; Tabata, C.; Ogawa, H.; Nakano, T.; Fujimori, Y. Deficiency of Fyn protein is prerequisite for apoptosis induced by Src family kinase inhibitors in human mesothelioma cells. *Carcinogenesis* **2012**, *33*, 969–975.
- (11) Singh, M. M.; Howard, A.; Irwin, M. E.; Gao, Y.; Lu, X. L.; Multani, A.; Chandra, J. Expression and Activity of Fyn Mediate Proliferation and Blastic Features of Chronic Myelogenous Leukemia. *PLoS One* **2012**, *7*, e51611.
- (12) Koo, J. H.; Lee, W. H.; Lee, C. G.; Kim, S. G. Fyn Inhibition by Cycloalkane-Fused 1,2-Dithiole-3-thiones Enhances Antioxidant Capacity and Protects Mitochondria from Oxidative Injury. *Mol. Pharmacol.* **2012**, *82*, 27–36.
- (13) Osterhout, D. J.; Wolven, A.; Wolf, R. M.; Resh, M. D.; Chao, M. V. Morphological differentiation of oligodendrocytes requires activation of Fyn tyrosine kinase. *J. Cell. Biol.* **1999**, *145*, 1209–1218.
- (14) Macurek, L.; Draberova, E.; Richterova, V.; Sulimenko, V.; Sulimenko, T.; Draberova, L.; Markova, V.; Draber, P. Regulation of microtubule nucleation from membranes by complexes of membrane-bound gamma-tubulin with Fyn kinase and phosphoinositide 3-kinase. *Biochem. J.* **2008**, *416*, 421–430.
- (15) Lim, S. H.; Kwon, S. K.; Lee, M. K.; Moon, J.; Jeong, D. G.; Park, E.; Kim, S. J.; Park, B. C.; Lee, S. C.; Ryu, S. E.; Yu, D. Y.; Chung, B. H.; Kim, E.; Myung, P. K.; Lee, J. R. Synapse formation regulated by protein tyrosine phosphatase receptor T through interaction with cell adhesion molecules and Fyn. *EMBO J.* **2009**, *28*, 3564–3578.
- (16) Kalia, L. V.; Salter, M. W. Interactions between Src family protein tyrosine kinases and PSD-95. *Neuropharmacology* **2003**, *45*, 720–728.
- (17) Chen, M.; Hou, X. Y.; Zhang, G. Y. Tyrosine kinase and tyrosine phosphatase participate in regulation of interactions of NMDA receptor subunit 2A with Src and Fyn mediated by PSD-95 after transient brain ischemia. *Neurosci. Lett.* **2003**, *339*, 29–32.
- (18) Lee, G. Tau and src family tyrosine kinases. *Biochim. Biophys. Acta, Mol. Basis Dis.* **2005**, *1739*, 323–330.
- (19) Lee, G.; Thangavel, R.; Sharma, V. M.; Litersky, J. M.; Bhaskar, K.; Fang, S. M.; Do, L. H.; Andreadis, A.; Van Hoesen, G.; Ksiezak-Reding, H. Phosphorylation of tau by fyn: Implications for Alzheimer's disease. *J. Neurosci.* **2004**, *24*, 2304–2312.
- (20) Bhaskar, K.; Hobbs, G. A.; Yen, S. H.; Lee, G. Tyrosine phosphorylation of tau accompanies disease progression in transgenic mouse models of tauopathy. *Neuropathol. Appl. Neurobiol.* **2010**, *36*, 462–477.
- (21) Um, J. W.; Nygaard, H. B.; Heiss, J. K.; Kostylev, M. A.; Stagi, M.; Vortmeyer, A.; Wisniewski, T.; Gunther, E. C.; Strittmatter, S. M. Alzheimer amyloid-beta oligomer bound to postsynaptic prion protein activates Fyn to impair neurons. *Nat. Neurosci.* **2012**, *15*, 1227–1235.
- (22) Larson, M.; Sherman, M. A.; Amar, F.; Nuvolone, M.; Schneider, J. A.; Bennett, D. A.; Aguzzi, A.; Lesne, S. E. The Complex PrPc-Fyn Couples Human Oligomeric A beta with Pathological Tau Changes in Alzheimer's Disease. *J. Neurosci.* **2012**, *32*, 16857–16871.
- (23) Du, C. P.; Tan, R.; Hou, X. Y. Fyn Kinases Play a Critical Role in Neuronal Apoptosis Induced by Oxygen and Glucose Deprivation or Amyloid-ss Peptide Treatment. *CNS Neurosci. Ther.* **2012**, *18*, 754–761.
- (24) Huang, H.; Ma, J.; Shi, J.; Meng, L.; Jiang, H.; Ding, J.; Liu, H. Discovery of novel purine derivatives with potent and selective inhibitory activity against c-Src tyrosine kinase. *Bioorg. Med. Chem.* **2010**, *18*, 4615–4624.
- (25) Lee, K.; Kim, J.; Jeong, K. W.; Lee, K. W.; Lee, Y.; Song, J. Y.; Kim, M. S.; Lee, G. S.; Kim, Y. Structure-based virtual screening of Src kinase inhibitors. *Bioorg. Med. Chem.* **2009**, *17*, 3152–3161.
- (26) Tuccinardi, T. Docking-based virtual screening: recent developments. *Comb. Chem. High Throughput Screening* **2009**, *12*, 303–314.
- (27) Rohrer, S. G.; Baumann, K. Maximum unbiased validation (MUV) data sets for virtual screening based on PubChem bioactivity data. *J. Chem. Inf. Model.* **2009**, *49*, 169–184.
- (28) Baroni, M.; Cruciani, G.; Sciabola, S.; Perruccio, F.; Mason, J. S. A common reference framework for analyzing/comparing proteins and

ligands. Fingerprints for Ligands and Proteins (FLAP): theory and application. *J. Chem. Inf. Model.* **2007**, *47*, 279–294.

(29) Hanke, J. H.; Gardner, J. P.; Dow, R. L.; Changelian, P. S.; Brissette, W. H.; Weringer, E. J.; Pollok, B. A.; Connelly, P. A. Discovery of a novel, potent, and Src family-selective tyrosine kinase inhibitor. Study of Lck- and FynT-dependent T cell activation. *J. Biol. Chem.* **1996**, *271*, 695–701.

(30) Rapecki, S.; Allen, R. Inhibition of human T cell activation by novel Src kinase inhibitors is dependent upon the complexity of the signal delivered to the cell. *J. Pharmacol. Exp. Ther.* **2002**, *303*, 1325–1333.

(31) Summy, J. M.; Trevino, J. G.; Lesslie, D. P.; Baker, C. H.; Shakespeare, W. C.; Wang, Y.; Sundaramoorthi, R.; Metcalf, C. A., III; Keats, J. A.; Sawyer, T. K.; Gallick, G. E. AP23846, a novel and highly potent Src family kinase inhibitor, reduces vascular endothelial growth factor and interleukin-8 expression in human solid tumor cell lines and abrogates downstream angiogenic processes. *Mol. Cancer Ther.* **2005**, *4*, 1900–1911.

(32) Das, J.; Chen, P.; Norris, D.; Padmanabha, R.; Lin, J.; Moquin, R. V.; Shen, Z.; Cook, L. S.; Doweiko, A. M.; Pitt, S.; Pang, S.; Shen, D. R.; Fang, Q.; de Fex, H. F.; McIntyre, K. W.; Shuster, D. J.; Gillooly, K. M.; Behnia, K.; Schieven, G. L.; Wityak, J.; Barrish, J. C. 2-Aminothiazole as a novel kinase inhibitor template. Structure-activity relationship studies toward the discovery of N-(2-chloro-6-methylphenyl)-2-[[6-[4-(2-hydroxyethyl)-1-piperazinyl]]-2-methyl-4-pyrimidinyl]amino]-1,3-thiazole-5-carboxamide (dasatinib, BMS-354825) as a potent pan-Src kinase inhibitor. *J. Med. Chem.* **2006**, *49*, 6819–6832.

(33) Bamborough, P.; Drewry, D.; Harper, G.; Smith, G. K.; Schneider, K. Assessment of chemical coverage of kinome space and its implications for kinase drug discovery. *J. Med. Chem.* **2008**, *51*, 7898–7914.

(34) Nathan Tumey, L.; Boschelli, D. H.; Lee, J.; Chaudhary, D. 2-Alkenylthieno[2,3-b]pyridine-5-carbonitriles: Potent and selective inhibitors of PKC θ . *Bioorg. Med. Chem. Lett.* **2008**, *18*, 4420–4423.

(35) Kinoshita, T.; Matsubara, M.; Ishiguro, H.; Okita, K.; Tada, T. Structure of human Fyn kinase domain complexed with staurosporine. *Biochem. Biophys. Res. Commun.* **2006**, *346*, 840–844.

(36) Cross, S.; Baroni, M.; Goracci, L.; Cruciani, G. GRID-based three-dimensional pharmacophores I: FLAPpharm, a novel approach for pharmacophore elucidation. *J. Chem. Inf. Model.* **2012**, *52*, 2587–2598.

(37) Verdonk, M. L.; Cole, J. C.; Hartshorn, M. J.; Murray, C. W.; Taylor, R. D. Improved protein-ligand docking using GOLD. *Proteins* **2003**, *52*, 609–623.

(38) Tuccinardi, T.; Botta, M.; Giordano, A.; Martinelli, A. Protein kinases: docking and homology modeling reliability. *J. Chem. Inf. Model.* **2010**, *50*, 1432–1441.

(39) FRED, version 2.2.5; OpenEye Scientific Software: Santa Fe, NM, USA, 2010.

(40) DOCK, version 6.0; Molecular Design Institute: University of California: San Francisco, CA, 1998.

(41) Dar, A. C.; Lopez, M. S.; Shokat, K. M. Small molecule recognition of c-Src via the Imatinib-binding conformation. *Chem. Biol.* **2008**, *15*, 1015–1022.

(42) Getlik, M.; Grutter, C.; Simard, J. R.; Kluter, S.; Rabiller, M.; Rode, H. B.; Robubi, A.; Rauh, D. Hybrid compound design to overcome the gatekeeper T338M mutation in cSrc. *J. Med. Chem.* **2009**, *52*, 3915–3926.

(43) Brandvold, K. R.; Steffey, M. E.; Fox, C. C.; Soellner, M. B. Development of a highly selective c-Src kinase inhibitor. *ACS Chem. Biol.* **2012**, *7*, 1393–1398.

(44) Buzzetti, F.; Brasca, M. G.; Crugnola, A.; Fustinoni, S.; Longo, A.; Penco, S.; Dalla Zonca, P.; Comoglio, P. M. Cinnamide analogs as inhibitors of protein tyrosine kinases. *Farmaco* **1993**, *48*, 615–636.

(45) Kim, A. N.; Jeon, W. K.; Lim, K. H.; Lee, H. Y.; Kim, W. J.; Kim, B. C. Fyn mediates transforming growth factor- β 1-induced down-regulation of E-cadherin in human A549 lung cancer cells. *Biochem. Biophys. Res. Commun.* **2011**, *407*, 181–184.

(46) Green, T. P.; Fennell, M.; Whittaker, R.; Curwen, J.; Jacobs, V.; Allen, J.; Logie, A.; Hargreaves, J.; Hickinson, D. M.; Wilkinson, R. W.; Elvin, P.; Boyer, B.; Carragher, N.; Plé, P. A.; Bermingham, A.; Holdgate, G. A.; Ward, W. H.; Hennequin, L. F.; Davies, B. R.; Costello, G. F. Preclinical anticancer activity of the potent, oral Src inhibitor AZD0530. *Mol. Oncol.* **2009**, *3*, 248–261.

(47) LigPrep, version 2.5; Schrödinger: New York, NY, 2011.

(48) Cross, S.; Baroni, M.; Carosati, E.; Benedetti, P.; Clementi, S. FLAP: GRID molecular interaction fields in virtual screening. Validation using the DUD data set. *J. Chem. Inf. Model.* **2010**, *50*, 1442–1450.

(49) Sirci, F.; Goracci, L.; Rodriguez, D.; van Muijlwijk-Koezen, J.; Gutierrez-de-Teran, H.; Mannhold, R. Ligand-, structure- and pharmacophore-based molecular fingerprints: a case study on adenosine A(1), A(2A), A(2B), and A(3) receptor antagonists. *J. Comput. Aided Mol. Des.* **2012**, *26*, 1247–1266.

(50) Case, D. A.; Darden, T. A., III; T., E. C.; Simmerling, C. L.; Wang, J.; Duke, R. E.; Luo, R.; Walker, R. C.; Zhang, W.; Merz, K. M.; Roberts, B.; Wang, B.; Hayik, S.; Roitberg, A.; Seabra, G.; Kolossváry, I.; Wong, K. F.; Paesani, F.; Vanicek, J.; Liu, J.; Wu, X.; Brozell, S. R.; Steinbrecher, T.; Gohlke, H.; Cai, Q.; Ye, X.; Wang, J.; Hsieh, M.-J.; Cui, G.; Roe, D. R.; Mathews, D. H.; Seetin, M. G.; Sagui, C.; Babin, V.; Luchko, T.; Gusarov, S.; Kovalenko, A.; Kollman, P. A. AMBER, version 11; University of California: San Francisco, CA, 2010.

(51) QUACPAC, version 1.5.0; OpenEye Scientific Software: Santa Fe, NM, USA, 2010.

(52) Lepp, Z.; Kinoshita, T.; Chuman, H. Screening for New Antidepressant Leads of Multiple Activities by Support Vector Machines. *J. Chem. Inf. Model.* **2006**, *46*, 158–167.

(53) SciFinder Scholar; American Chemical Society: Washington, DC, 2013.

(54) Asinex. <http://www.asinex.com/index.html> (accessed Oct 14, 2012).

(55) Tocris Bioscience. <http://www.tocris.com/> (accessed Nov 4, 2012).

(56) Promega Corporation. www.promega.com/ (accessed Nov 10, 2012).

(57) ProQinase GmbH. www.proqinase.com/ (accessed June 18, 2013).